UNIVERSITY OF LEEDS

Parametric study of CO$_2$ methanation for synthetic natural gas production

Mohammad M. Jaffar, Mohamad A. Nahil, Paul T. Williams[*]

School of Chemical and Process Engineering, University of Leeds, Leeds, LS2 9JT, U.K.

([*]Corresponding author; Email; p.t.williams@leeds.ac.uk; Tel; #44 1133432504)

ABSTRACT: The production of methane through carbon dioxide hydrogenation through optimization of the operating parameters to enhance methane yield and carbon dioxide conversion in a two-stage fixed bed reactor has been investigated. The influence of temperature, gas flow rate (GHSV) and H$_2$:CO$_2$ ratio on the production of methane was undertaken. In addition, different methanation catalysts in terms of metal promoters and support materials were investigated to maximize methane production. The results showed that the maximum methane yield and maximum carbon dioxide conversion was obtained at a catalyst temperature of 360 °C with a H$_2$:CO$_2$ ratio of 4:1 and total gas hourly space velocity of 6000 ml h^{-1} g^{-1}$_{catalyst}$ and reactant gases hourly space velocity of 3000 ml h^{-1} g^{-1}$_{catalyst}$. The optimum metal-alumina catalyst investigated for CO$_2$ conversion and methane yield was 10wt.%-Ni/Al$_2$O$_3$ catalyst. However, reduction in the methane yield was observed with the addition of the Fe and Co promotors because of catalyst sintering and non-uniform dispersion of metals on the support. Among the different catalyst support materials studied i.e. Al$_2$O$_3$, SiO$_2$ and MCM-41 the highest catalytic activity was shown by the Al$_2$O$_3$ catalyst with 83 mol.% CO$_2$ conversion, producing 81 mol.% CH$_4$ with 98% CH$_4$ selectivity.

Key words: Carbon dioxide; Methanation; Catalyst; Hydrogenation; Methane

1. INTRODUCTION

Currently with the growing environmental impact and cost of energy production via fossil fuels, interest is now growing in renewable energy. Carbon dioxide is the major greenhouse gas produced by combustion of various fossil fuels and has a major role in the increase in the temperature of the earth's atmosphere. In order to overcome this dilemma, there is a move towards low carbon emissions via the use of carbon-neutral fuels.[1]

Catalytic reactions of H_2 and CO_2 (hydrogenation) have been used to produce a range of useful fuels and chemicals, including, methane, gasoline range hydrocarbons, C_2 — C_2 alkenes, organic acids, methanol and other alcohols.[2] There is particular interest in the production of methane from the catalytic hydrogenation process, i.e. methanation (Reaction 1). [2,3]

$$CO_2 + 4H_2 \rightarrow CH_4 + 2H_2O \text{ (Methanation Reaction)} \tag{1}$$
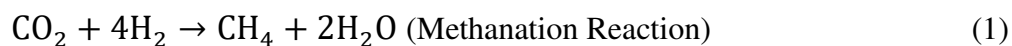
However, the mechanism of the CO_2 methanation reaction remains unclear.[4] Some studies have suggested the reverse water gas shift (RWGS) reaction (Reaction 2) as an intermediate reaction in the production of methane by CO_2 hydrogenation. The produced CO from the RWGS reaction reacts with the H_2 to produce methane (Reaction 3).[5] Alternatively, some studies have assumed that the produced CO and CH_4 are the product of two parallel reactions (1) and (2).

$$CO_2 + H_2 \rightarrow CO + H_2O \text{ (RWGS Reaction)} \tag{2}$$

$$CO + 3H_2 \rightarrow CH_4 + H_2O \tag{3}$$

It has been shown that the methanation reaction is dependent on several factors i.e. temperature, pressure, reactant gas composition (CO_2: H_2 ratio).[6-8] For example, because the methanation reaction is exothermic, lower temperatures favors the reaction [6] and a typical operational temperature range for methane production is from 200 – 500 °C [8,9]. Reaction (1) indicates that from Le Chatelier's principle, higher pressures (typically in the range 0.2-0.3 MPa) favors CO_2 methanation to produce methane.[9] Thermodynamic analysis has therefore revealed that higher pressures and lower temperature are the ideal conditions for the methanation reaction.[10,11]

The use of catalysts can enhance the CH_4 selectivity from CO_2 methanation. Extensive studies have been carried out to optimise methane production using heterogeneous VIIIB group metal based catalysts such as Ni, Fe, Co, Ru, Rh, Pt, Pd on different support materials (Al_2O_3, SiO_2, ZrO_2, CeO_2, TiO_2).[12] Efficient catalytic activity and methane selectivity were observed with Ru [13], Rh [14] and Ni [15] based catalysts. Nickel supported catalysts, because of their cost-effectiveness and high catalytic activity, have been widely used for CO_2 hydrogenation to produce methane.[16]

This paper reports on an investigation into the optimized production of methane from H_2 and CO_2 gases via catalytic methanation. The main objective of this research was to study and optimize the operating parameters for methane production. Various operating parameters, which included N_2 gas flow rate, catalyst temperature, H_2:CO_2 ratio, the use of different metal-alumina catalysts, catalyst calcination temperature, the role of different catalyst support materials and the effect of different metal catalyst promotors on the Ni-alumina catalyst were investigated to maximise the production of methane.

2. MATERIALS AND METHODS

2.1 Catalyst Preparation: To investigate the influence of operating parameters on the production of methane via the methanation reaction, a 10 wt.%-Ni/Al_2O_3catalyst was used. In addition, different 10 wt.%-metal-alumina catalysts were prepared and different metal promoted Ni-alumina catalysts were investigated. The influence of the catalyst support materials using a 10 wt.%-Ni supported catalysts were also investigated.

For 10 wt.%-Ni/Al_2O_3 catalyst preparation; Al_2O_3 was crushed and then sieved to obtain alumina of a size range of 50-212 µm. 10 wt.%-Ni/Al_2O_3 was prepared by a wet impregnation method. Nickel nitrate hexa- hydrate $Ni(NO_3)_2.6H_2O$ was dissolved in distilled water to obtain an aqueous solution. The alumina was then mixed in the $Ni(NO_3)_2.6H_2O$ aqueous solution and stirred for several hours with an increase in temperature of 15 °C every 30 min until the water evaporated. The paste obtained was then dried overnight at 105 °C and the dried sample was calcined at 750 °C in a furnace. The obtained calcined sample was crushed and sieved to obtain catalyst particle size range of 50-212 µm. Sieved catalyst was finally reduced at 800 °C in a reduction furnace under H_2 atmosphere (5 % H_2 and 95 % N_2) for 2 h.

To investigate the effect of other metal-alumina catalysts at the optimized process conditions obtained with the 10 wt.%-Ni/Al_2O_3 catalyst, various metal catalysts were studied.

10 wt.% of Fe, Co and Mo on alumina (Al_2O_3) support were prepared to obtain 10 wt.%-Fe/Al_2O_3, 10wt.%-Co/Al_2O_3 and 10wt.%-Mo/Al_2O_3 catalysts respectively. All these metal-based Al_2O_3 catalysts were prepared by the wet impregnation method described above. Iron (III) nitrate nano hydrate, cobalt (II) nitrate hexa-hydrate, ammonium molybdate (para) tetra hydrate precursor salts were impregnated on Al_2O_3 to obtain the 10 wt.%-Fe/Al_2O_3, 10 wt.%-Co/Al_2O_3 and 10 wt.%-Mo/Al_2O_3 catalysts respectively. After drying, the catalysts were calcined at 950 °C and reduced with hydrogen at 800 °C for 2 h.

For the investigation of the influence of metal promotors on the Ni/Al_2O_3 catalyst, Fe and Co metals were used. The precursors for Fe and Co catalysts were iron (III) nitrate nano hydrate and cobalt (II) nitrate hexa-hydrate added to 10 wt.%-Ni/Al_2O_3 to produce the desired metal loading a t different wt.% metal for the catalysts. The different metal loadings investigated were, 10 wt.%-Ni/ 3 wt.%-Fe-Al_2O_3, 10 wt.%-Ni/3 wt.%-Co-Al_2O_3, 7 wt.%-Ni/ 3 wt.% Co-Al_2O_3 and 10 wt.%-Ni/ 1 wt.%-Co-Al_2O_3. The prepared catalysts were dried, calcined at 950 °C and reduced at 800 °C. For During the mass of nickel loaded onto the alumina support was also investigared at three different Ni loadings of 5 wt.%, 10 wt.% and 15 wt.% each prepared by the wet impregnation method as before. The precursor for nickel was nickel nitrate hexa- hydrate. To investigate the influence of different support materials on the methanation process, suitable amounts of SiO_2 and MCM-41 were added separately to nickel nitrate hexa- hydrate solution to make 10 wt.%-Ni/SiO_2 and 10 wt.%-Ni/MCM-41 catalysts, in addition to the 10 wt.%-Ni/Al_2O_3 catalyst. Each of the prepared catalysts were calcined at 950 °C and reduced with hydrogen at 800 °C for 2 h

2.2 Catalytic methanation reactor system: A fixed bed catalytic reactor was used to carry out the catalytic methanation reaction experiments, involving a gas pre-heater and catalytic reactor. A schematic diagram of the methanation reactor is shown in Figure 1. The gas pre-heater was 25 cm x 5 cm diameter and catalytic reactor was 32 cm x 2 cm diameter both constructed of cylindrical stainless steel tubes and were heated using separately controlled electric furnaces. The temperatures of the gas pre-heater and catalyst bed were monitored by thermocouples. Hydrogen reactant gas was produced by a Packard 9200 hydrogen generator (Sigma-Aldrich) at 99.9999% H_2 purity. CO_2 and N_2 were supplied by gas cylinders from BOC Ltd., UK at 99.995% and 99.999% gas purity respectively. All gases were metered and passed to the reactor via a gas mixer. Condensers were attached to the output of the reactor to capture the water produced by the methanation reaction via water-cooled and solid dry-ice (CO_2)

cooled condensers. After the condensers, the non-condensable gases were collected in a 25 L Tedlar™ gas sample bag for later analysis by packed column gas chromatography. The experimental procedure was to first heat the catalyst reactor to the desired catalyst temperature and the gas pre-heater to 360 °C, the reactant gases were then introduced to the reactor system. The process parameters investigated using the 10 wt.%-Ni-Al$_2$O$_3$ catalyst were; reactant gas weight hourly space velocity of 1200, 1600, 2400, 3000, 3600, 4200 and 4800 ml h^{-1} g^{-1}$_{catalyst}$; catalyst temperature at 240, 280, 320, 360 and 400 °C; reactant gas, H$_2$:CO$_2$ ratio of 2:1, 3:1, 4:1 and 4.5:1. In addition, the catalyst preparation calcination temperature at 550, 650, 750, 850 and 950 °C were investigated to determine the influence on methane production. Also, the influence of Fe and Co as catalyst metal promoters added to the Ni-Al$_2$O$_3$ catalyst and also the influence of different catalyst support materials was investigated. Experiments were repeated with excellent mass balances obtained for the experiments.

The carbon dioxide conversion, methane yield and methane selectivity was calculated by the following formulas.

$$CO_2 \text{ Conversion } (\%) = \frac{CO_2 \text{ reacted (mols)}}{CO_2 \text{ input (mols)}} \times 100 \qquad (4)$$

$$CH_4 \text{ Yield } (\%) = \frac{CH_4 \text{ output (mols)}}{CO_2 \text{ input (mols)}} \times 100 \qquad (5)$$

$$CH_4 \text{ Selectivity } (\%) = \frac{CH_4 \text{ output (mols)}}{CO_2 \text{ reacted (mols)}} \times 100 \qquad (6)$$

2.3. Gas analysis: The gases produced from the catalytic methanation reaction collected in the gas sample bag were analysed immediately after each experiment. Permanent gases, CO, H$_2$, N$_2$ and O$_2$, were analysed by a Varian CP 3330 gas chromatograph (GC) using a HayeSep 60-80 mesh molecular sieve column, with Ar carrier gas and a thermal conductivity detector (TCD). Because of similar retention times for CO and CO$_2$, CO$_2$ was analysed separately with a second Varian CP 3330 GC, also with a 60-80 mesh molecular sieve GC column, Ar carrier gas and TCD but with different chromatographic conditions. Methane was analysed using a Varian CP-3380 gas chromatograph having a 80-100 mesh HayeSep column with flame ionization detector and N$_2$ as a carrier gas.

2.4. Catalyst characterisation: The prepared catalysts were characterized by powder X-ray diffraction (XRD) determined using a Bruker D8 powder X-ray diffractometer, with CuKα radiation at 40 kV and 40 mA. The crystal size of the metal catalyst particles was calculated using the Scherrer equation.[17] In addition, the surface morphologies of the catalysts

were determined by scanning electron microscopy (SEM). The SEM system used was a Hitachi SU8230 operated at 20 kV. In addition, elemental mapping of the catalysts was obtained with energy dispersive X-ray spectroscopy (EDXS) which was closely coupled to the SEM.

3. RESULTS AND DISCUSSION

3.1 Influence of reactant gases hourly space velocity

The influence of gas hourly space velocity of the reactant gases on the formation of methane was investigated at 1200 to 4800 ml h^{-1} $g^{-1}_{catalyst}$ space velocities using the 10 wt.%-Ni-Al_2O_3 catalyst while maintaining the $H_2:CO_2$ ratio at 4:1. A total gas (reactant gases plus nitrogen) hourly space velocity of 6000 ml h^{-1} $g^{-1}_{catalyst}$ was used, where nitrogen was used as the balance gas. The catalyst temperature was maintained at 340 °C for these experiments, since this has been reported to be the optimum temperature for methanation by Zhou et al., [18] using Ni/CeO_2 as a catalyst in a quartz tube, fixed bed reactor with a continuous flow of reactant gases. The temperature range that they investigated was between 260-340 °C in relation to the CO_2 methanation reaction. The most effective catalytic activity was observed at the temperature of 340 °C. They reported that a lower temperature i.e. 260 °C was not favorable to form active $H^{\bullet}$ radical species from H_2 which ultimately takes part in the CO_2 methanation reaction. Figure 2 shows the effect of different reactant gases hourly space velocity on methane production. The results suggested that the maximum methane yield, methane concentration, and carbon dioxide conversion was obtained with 3000 ml h^{-1} $g^{-1}_{catalyst}$. It was observed that when the reactant gas space velocity was increased from 1200 to 3000 ml $h^{-1}g^{-1}_{catalyst}$, the methane yield increased from 48.6 to 54.9 mol.%, methane concentration increased from 2.6 to 7.4 mmol., methane selectivity increased from 91.21 to 95.54 mol.% and carbon dioxide conversion increased from 53.3 to 57.6 mol.%. Increasing the gas hourly space velocity of the reactants supplied the feedstock gases to the catalyst to facilitate the methanation reaction up to an optimum at ~3000 ml h^{-1} $g^{-1}_{catalyst}$. But, with the further increase in the reactant gases hourly space velocity to 4800 ml h^{-1} $g^{-1}_{catalyst}$, the methane yield, methane concentration, methane selectivity and carbon dioxide conversion reduced significantly to 25.8 mol.%, 5.5 mmol, 94.8% and 27.3 mol.% respectively. The results reported by Rahmani et al., [19] using a Ni/Al_2O_3 catalyst in a fixed bed

reactor are consistent with our studies. They conducted the CO_2 methanation reaction at various gas space velocities in the range of 6000 - 18000 ml h^{-1} $g^{-1}_{catalyst}$. They reported that a, higher GHSV results in reduced contact time between the catalyst and the reactant gases, as a result lesser amounts of reactant gases are absorbed on the catalyst which results in a lower conversion. This decrease in the methanation activity with increase in reactant gases was also reported by Vita et al.[20] The effect of reactant gas space velocity on the CO_2 methanation reaction was investigated using a quartz tube, fixed bed reactor in the range of 10000 - 50000 h^{-1} $g^{-1}_{catalyst}$. The most effective catalytic activity and the highest methane concentration produced was observed at the 10000 h^{-1} $g^{-1}_{catalyst}$ space velocity. They reported that an increase in gas space velocity would result in a shorter time of contact between the catalyst and the gases and consequently a reduction in conversion. Other researchers have studied the relationship between temperature and the space velocity of the gases. For example, Abate et al., [21] studied the effect of gas space velocity and the catalyst temperature in a quartz reactor using a Ni-Al hydrotalcite catalyst. Gas hourly space velocities of 20000 h^{-1} $g^{-1}_{catalyst}$, 25000 h^{-1} $g_{catalyst}$, 30000 h^{-1} $g^{-1}_{catalyst}$ over the temperature range of 250- 400 °C were investigated. They showed that with the increase in the gas space velocity, methane yield decreased and this trend was clearer at lower temperature (far from the chemical equilibrium). However, with the increase in temperature, this trend became diminished because of the chemical equilibrium. Similarly, Ocampo et al., [22] studied the effect of catalyst temperature over the range of 200- 400 °C on the gas space velocity range of 2100-64000 h^{-1} g^{-1} $_{catalyst}$ using a Ni/Ce$_{0.72}$ Zr$_{0.28}$ O$_2$ catalyst in a fixed bed, down flow reactor. They reported that higher gas space velocities resulted in lower CO_2 conversion to methane. At lower temperatures i.e. 200 and 250 °C CO_2 conversion remained the same at different space velocities but the trend was clearly visible at the higher reaction temperatures i.e. 300, 350, and 400 °C. Moghaddam et al., [23] studied the effect of space velocity within the range of 6000 – 8000 ml h^{-1} $g^{-1}_{catalyst}$ at 350 °C for CO_2 methanation using Ni/Al$_2$O$_3$-SiO$_2$ catalyst in a quartz micro reactor. They reported that the CO_2 conversion decreased with the increase in gas space velocity because of the shorter contact time and the decrease in the adsorbed reactant content on the surface of the catalyst.

However, it should also be noted that most of the studies focus on the total space velocity of all the gases including nitrogen, hydrogen and carbon dioxide, but, there is less literature available in relation to the effect of space velocity of the reactant gases only.

3.2 Influence of catalyst temperature

The influence of the catalyst temperature on the CO_2 conversion, methane selectivity and methane yield for the carbon dioxide methanation reaction was undertaken at catalyst temperatures of 240, 280, 320, 360 and 400 °C. The catalyst used was 10 wt.%-Ni/Al_2O_3 with a H_2:CO_2 ratio of 4:1. The total gas hourly space velocity (GHSV) during the reaction was maintained at 6000 ml h^{-1} $g^{-1}_{catalyst}$ and reactant gases hourly space velocity was 3000 ml $h^{-1}g^{-1}_{catalyst}$. The results are shown in Figure 3. It was observed that with the initial increase in temperature, the CO_2 conversion increased also methane selectivity increaed. Methanation of CO_2 is an exothermic reaction so it is favorable at a lower temperature. The maximum CO_2 conversion of 72.1 mol. % was obtained when the temperature was increased from 240 °C to 360 °C. At 360 °C maximum methane yield of 69.2 mol.% and maximum selectivity of 96.1 % was observed. At 400 °C catalyst temperature, the decrease in methane yield and selectivity indicates enhancement of the reverse water gas shift reaction, as the CO concentration in the product gases increased. Also, the results reported here show that the selectivity of methane was 100% at lower catalyst temperature i.e. <320 °C. No CO was observed at lower temperatures, however, with the increase in the catalyst temperature CH_4 selectivity decreased with the formation of CO. However, the maximum methane yield was observed at the catalyst temperature of 360 °C. At the catalyst temperature of 400 °C the RWGS (reverse water gas shift reaction) reaction suppressed the methanation reaction by enhancing the CO and reducing the CH_4 formation. Rahmani et al., [19] investigated the influence of temperature on the CO_2 methanation reaction using various nickel loadings on a Al_2O_3 support in a fixed bed reactor. They studied the behavior of a Ni/Al_2O_3 catalyst with various nickel loadings in the temperature range of 200 – 500 °C. They reported that the maximum carbon dioxide conversion into methane occurred at a lower temperature i.e. 350 °C but, with the increase in temperature the reverse water gas shift reaction becomes dominant. As a result, methane yield decreases, resulting in an increase in CO selectivity at higher temperature. A similar trend was observed for all the catalysts investigated with the various nickel loadings that they used. Similar results were reported by Jia et al., [24] using a Ni/ZrO_2 catalyst for CO_2 methanation in a horizontal quartz tube, fixed bed reactor. They studied CO_2 methanation in the temperature range of 200 - 400 °C. According to their results the CH_4 selectivity was a maximum at lower temperature i.e. <270 °C however, with the increase in temperature selectivity decreased because of the

reverse water gas shift reaction. The maximum CH_4 yield and CO_2 conversion was observed at a catalyst temperature of 350 °C but, with the further increase in temperature CH_4 yield and CO_2 conversion diminished because of thermodynamic equilibrium limitations. It has been reported by Stangeland et al., [9] that CO_2 conversion increases dramatically above 325 °C with a Ni/Al_2O_3 catalyst using a fixed bed tubular reactor. They reported that CO_2 conversion was theoretically possible at lower temperatures but, higher temperature is favorable because of the associated difficulties with CO_2 activation and slow reaction kinetics at lower temperature.

3.3. Influence of H_2:CO_2 ratio

The influence of the H_2:CO_2 ratio on the methanation reaction were investigated. The reactant H_2 and CO_2 ratios were changed by varying the independent input flow rates of H_2 and CO_2, to produce H_2:CO_2 ratios of 2:1, 3:1, 4:1 and 4.5:1. The catalyst used was, 10wt.%-Ni/Al_2O_3 and the reaction conditions were maintained at a catalyst temperature of 360°C, a total gas hourly space velocity of 6000 ml h^{-1} $g^{-1}_{catalyst}$ while the reactant H_2 and CO_2 gas hourly space velocity (RGHSV) was 3000 ml h^{-1} $g^{-1}_{catalyst}$. The results of methane yield and concentration, carbon dioxide conversion and methane selectivity in relation to H_2:CO_2 ratio is shown in Figure 4. It can be seen that the H_2:CO_2 ratio greatly influences the carbon dioxide conversion, methane yield, and selectivity of the methane product. At the higher H_2:CO_2 ratio of 4:1, the results show a higher CO_2 conversion and high methane yield. For example, when the H_2:CO_2 ratio was increased from 2:1 to 4:1, carbon dioxide conversion and selectivity of methane increased from 29.1 mol.% to 71.7 mol.% and 88.9% to 96.1% respectively. Also, methane concentration increased from 5.8 mmol to 9.3 mmol with the increase in the H_2:CO_2 ratio. However, at the highest H_2:CO_2 ratio of 4.5:1, the CO_2 conversion and CH_4 yield decreased. Other researchers have investigated the CO_2 methanation reaction in relation to H_2:CO_2 ratio and shown a similar effect. For example, Aziz et al., [8] studied the influence of H_2:CO_2 ratio at a catalyst temperature of 300 °C using a Ni/MSN (nickel-mesoporous silica nano-spheres) catalyst in a quartz fixed bed reactor. They reported that the optimum H_2:CO_2 ratio for CO_2 methanation was 4:1 and it decreased with the increase in ratio to 7:1. They suggested that the trend of catalytic activity was because of the variation of hydrogen concentration in the reactant gases. Optimum hydrogen adsorbs on the catalyst surface and at the same time hydrogenates the carbonated species, resulting in conversion to methane. Similarly, Moghaddam et al., [23] studied the effect of H_2:CO_2 molar ratio within the range of 3:1 to 4:1 at a catalyst temperature of 350 °C for CO_2 methanation using a $Ni/Al_2O_3/SiO_2$ catalyst in a quartz micro reactor. They reported the

maximum CH_4 yield and maximum CO_2 conversion was observed at the H_2:CO_2 molar ratio of 4:1. It was suggested that the reason behind the maximum conversion at these conditions is the presence of a sufficient amount of hydrogen for hydrogenating the carbonate species formed during the reaction. They also reported that there was a negligible effect of molar ratio of 3.5:1 and 4:1 on selectivity because almost all of the CO_2 converts into methane at a molar ratio of 3.5:1 at 350 °C. Also, comparable results have been reported by Zhou et al., [25] using a a fixed bed reactor with a $Ni/Al_2O_3/CeO_2$ catalyst at 400 °C temperature and H_2:CO_2 molar ratio within the range of 1:1 to 7:1. Their simulation results and experimental results showed that the CO_2 conversion and CH_4 selectivity increased with the increase in molar ratio. However, the selectivity of CH_4 increased further with the increase in molar ratio even above 4:1 but the maximum CO_2 conversion was observed at the molar ratio of 4:1. It may be concluded, that most studies have reported that the ideal H_2:CO_2 molar ratio for the methanation reaction is 4:1. However, some studies have shown that excess hydrogen has a significant effect on the pathway of the specific reaction.[26] The results shown here suggest that, to obtain higher methane concentrations and higher carbon dioxide conversion, an optimum H_2:CO_2 ratio of 4:1 is required.

3.4. Influence of catalyst metal

Catalytic activity and selectivity using various metals on an alumina support were investigated for the CO_2 methanation reaction. The catalysts compared were, 10wt.%-Ni/Al_2O_3, 10wt.%-Fe/Al_2O_3, 10wt.%-Co/Al_2O_3 and 10wt.%-Mo/Al_2O_3. The catalyst temperature was maintained at 360 °C, the H_2:CO_2 ratio at 4:1 and the total gas hourly space velocity (TGHSV) was 6000 ml $h^{-1}g^{-1}_{catalyst}$. The reactant gases hourly space velocity (RGHSV) was 3000ml $h^{-1}g^{-1}_{catalyst}$. The results are shown in Table 1. Among all the catalysts investigated, the Ni/Al_2O_3 catalyst showed the highest catalytic activity and selectivity. The activity of the catalysts at optimized conditions decreased in the order Ni>Co>Fe>Mo. The nickel and cobalt alumina catalysts showed the highest carbon dioxide conversion of 72.1 mol.% and 50.3 mol.% respectively and maximum selectivity of 96.1 % and 81.1 % respectively. However, the Fe and Mo catalysts showed an activity and selectivity for methane production which was much less as compared to the nickel and cobalt containing catalysts.

Other reports have investigated the influence of the catalyst metal on the methanation reaction. For example, the activity of different metal catalysts on an MSN support under

methanation conditions was studied by Aziz et al., [27]. They reported that different metal catalysts have different activity at different temperature ranges. An Fe catalyst had no catalytic effect at lower temperature (<350 °C), but at higher temperature its activity increased, but, the activity was far less than a nickel catalyst which was also active at lower temperatures. It was reported that the activity of the Fe catalyst was greater than for Mo. According to experiments performed by Razzaq et al., [28] in a fixed bed quartz reactor, the most effective catalytic activity was shown by a Co/Al_2O_3 catalyst at a lower temperature range (200-250 °C) along with the formation of higher hydrocarbons. But, with the increase in temperature to 350 °C, CH_4 yield and the formation of other hydrocarbons was suppressed. Therefore, the activity of the catalysts varies with the temperature ranges used. Similarly, it has been reported by Aksoylu et al., [29] that the CO_2 methanation activity of molybdenum based catalysts are almost negligible even with higher molybdenum loading at 250 °C. However, they suggested that molybdenum can be used as a promotor with a nickel catalyst to enhance the methanation activity. They performed experiments using a molybdenum promoted Ni/Al_2O_3 catalyst to enhance the catalytic activity for the methanation reaction. The enhancement of the catalytic activity was observed with low percentage of molybdenum loading on the nickel alumina catalyst. Also, the effect of iron as a catalyst promoter on a Ni/Al_2O_3 catalyst was investigated by Burger et al., [30] in the temperature range of 150- 400 °C. According to their results it was shown that the addition of Fe to Ni/Al_2O_3 had a positive effect on the enhancement of CO_2 conversion. They studied various loadings of Fe (2%, 4%, 7% and 10%) on the Ni/Al_2O_3 catalyst and showed that CO_2 conversion was increased with the increase in Fe content from 2 - 7 wt.%. However with the further increase of Fe to 10% CO_2 conversion reduced.

3.5. Influence of catalyst calcination temperature

The influence of calcination temperature on the crystal structure of the produced 10 wt.%-Ni/Al_2O_3 catalysts was investigated using XRD. The XRD results of the catalysts in relation to different calcination temperatures is shown in Figure 5. The increase in calcination temperature from 550 °C to 950 °C showed that the alumina and nickel XRD diffraction peaks appeared with increased intensity. An increase in the metal particle size was also observed with the increase in calcination temperature as calculated using the Scherrer equation.[17] The Ni particle size increased from 1.8 nm to 12.3 nm with the increase in calcination temperature from 550 °C to 950 °C. The crystalline phase of alumina indicated by the XRD diffraction also becomes

more intense at higher calcination temperature. There was only a single visible XRD diffraction peak observed at 550 ºC calcination temperature having diffraction peak of 2-theta at 66.42º. With the increase in calcination temperature to 950 ºC various alumina XRD diffraction peaks appeared at 2 theta at 39.2º, 66.42º, 19.13º, 31.6º, 45.5º and 60.34º.

The catalysts prepared using different calcination temperatures were investigated to determine the influence on the methanation reaction. The effect on the catalytic activity and selectivity of CO_2 conversion and methane yield in relation to calcination temperature using the 10 wt.%-Ni-Al_2O_3 catalyst at the catalyst temperature of 360 °C was investigated. The H_2:CO_2 ratio was maintained at 4:1 with a TGHSV of 6000 ml $h^{-1}g^{-1}_{catalyst}$ and reactant gases hourly space velocity (RGHSV) of 3000 ml $h^{-1}g^{-1}_{catalyst}$. The 10 wt.%-Ni/Al_2O_3 catalyst was prepared over the temperature range of 550 °C to 950 °C. The results are shown in Figure 6. The results showed that the calcination temperature influenced the catalytic activity of the prepared 10 wt.%-Ni/Al_2O_3 catalyst and showing enhanced activity with the increase in calcination temperature. It was observed that the CO_2 conversion increased from 63.7 mol.% to 82.9 mol.%, selectivity increased from 95.0% to 97.9%, methane yield increased from 60.5 mol.% to 81.2 mol.% and the methane concentration from 8.1 mmol to 10.8 mmol respectively. Gao et. al., [31] studied the effect of various catalyst calcination temperatures (600, 800, 1000 and 1200 ºC) with a Ni/Al_2O_3 catalyst. They reported that an increase in the calcination temperature resulted in an increase in particle size of the metallic nickel. It was reported that larger particle sizes resulted in higher resistance to oxidation of the nickel particles. Their temperature programmed oxidation results of the Ni/Al_2O_3 catalyst calcined at 600 ºC showed the lowest resistance to oxidation and oxidized at lower temperature as compared to higher calcination temperatures. It therefore may be suggested that the larger crystal size of the metal results in increased resistance to oxidation of the metallic specie in the catalyst. Also, XRD data showed that the increase in Ni crystal size was linked with increased calcination temperature. Therefore, higher calcination temperatures are favorable for the methanation reaction.

3.6. Influence of catalyst metal loading

The effect of the increase in metal loading in the Ni-Al_2O_3 catalyst in relation to the methanation reaction was investigated. Initial work involved the analysis of the prepared catalyst using SEM and EDXS metal analysis of the catalysts to determine the extent of metal dispersion on the

catalyst. The results are presented in Figure 7 and Figure 8. The SEM-EDXS analysis shows that the NiO particles are more uniformly dispersed in the 5 wt.%-Ni loaded catalyst than in the 15 wt.% Ni-Al$_2$O$_3$ loaded catalyst. In addition, the SEM results indicate that the particle sizes of the 15 wt.%-Ni-Al$_2$O$_3$ loaded catalyst was greater than the 5 wt.%-Ni-Al$_2$O$_3$ loading. Thus, it can be concluded that with the increase in the nickel particle size, the uniform dispersion of the NiO particles on the support decreased and results in non-uniform dispersion of the nickel particles on the alumina support.

The XRD analysis of the nickel alumina catalysts with different nickel content is shown in Figure 9. In all the catalysts investigated, diffraction peaks at 2 theta, 37.4^o, 44.3^o, 51.68^o and 76.24^o showed the presence of metallic nickel in the reduced catalyst. Diffraction peaks at 2 theta, 39.2, 31.6^o, 45.5^o, 60.34^o and 66.42^o represent the alumina phase related diffraction peaks. It can be seen that the nickel diffraction peaks become more intense with the increase in nickel content from 5 wt.%-to 15 wt.%-loading. It can be seen that the crystalline structure of the nickel catalyst is strongly dependent on the nickel percentage on the support. In addition, the average particle size of the catalysts with different nickel content was calculated using the XRD analysis. The average particle size of the 5 wt.%, 10 wt.% and 15 wt.%-nickel-alumina catalysts was 7.0 nm, 10.2 and 12.3 nm. Increased nickel content increased the particle size which resulted in non-uniform dispersion of the nickel on the support.

The influence of nickel metal loading on the methanation reaction was investigated using the catalytic reactor system. The catalyst temperature was maintained at a temperature of 360 °C using the Ni-Al$_2$O$_3$ catalysts which were calcined at 950 °C. The molar ratio of H$_2$:CO$_2$ was kept constant at 4:1 and the TGHSV during the methanation reaction was 6000 ml h^{-1}g^{-1}$_{catalyst}$. The reactant gases hourly space velocity (RGHSV) was 3000 ml h^{-1}g^{-1}$_{catalyst}$. The results are shown in Figure 10. It was observed that the catalytic activity increased with the increase in metal loading initially and then decreased with the further increase. Among the various metal loadings studied, the highest catalytic activity was observed with the 10 wt.%-Ni/Al$_2$O$_3$ catalyst. Daroughegi et al., [32] studied the effect of various nickel loadings (15, 20, 25 and 33 wt. %) on an alumina supported catalyst for CO$_2$ methanation at different temperatures in a quartz fixed bed reactor. Their results showed that the increase in Ni loading resulted in an increase in particle size. In addition, an increase in nickel loading from 15 - 20 wt.% resulted in an increase in surface area, however, with the further increase in nickel loading to 33 wt.% the surface area decreased. They showed that CO$_2$ conversion was enhanced with increased nickel percentage in the catalyst from 15- 25 wt. % but, with further increase in nickel loading,

conversion and selectivity reduced because of reduced nickel dispersion. Also, Rahmani et al., [19] studied the effect of various loading of nickel on a alumina support in relation to CO_2 methanation at different catalyst temperatures. They also reported an initial increase and final decrease of the catalytic activity with increased metal loading. They reported that with the increase in nickel percentage from 10 - 15 wt.%, CO_2 conversion increased but a further increase in metal loading to 20 % resulted in a decrease in CO_2 conversion. According to their study, the increased metal loading resulted in decreased nickel dispersion on the support that resulted in increased metal crystal size, which in turn lowered the catalytic activity of the catalyst and resulted in lower CO_2 conversion. Zhen et al., [33] studied the effect of nickel loading on an MOF-5 catalyst at a catalyst temperature of 280 °C with a metal loading between 5.0 and 12.5 wt.% to determine the influence on CO_2 methanation. Their results suggested that with the increase in nickel loading from 5 - 10 wt.% the CO_2 conversion increased because of the provision of greater metal active sites. While higher nickel loading (>10 wt.%) resulted in the decrease in CO_2 conversion because of the segregation of metallic nickel particle resulting in diminished catalytic activity.

3.7 Influence of metal promotors with the Ni-alumina catalyst

The influence of the addition of metal catalyst promoters in the form of Fe and Co added to the Ni-Al_2O_3 catalyst in relation to methane production was investigated. The Fe, Co nickel catalysts investigated were; 10 wt.%-NiAl_2O_3/3wt.%-Fe/Al_2O_3, 10% wt.%Ni-Al_2O_3/3 wt.%-Co/Al_2O_3 and 7 wt.% Ni-Al_2O_3/ 3 wt.%-Co/Al_2O_3. The reaction temperature was maintained at 360 °C, the H_2:CO_2 ratio was 4:1, the TGHSV was 6000 ml $h^{-1}g^{-1}_{catalyst}$ and the RGHSV was 3000 ml $h^{-1}g^{-1}_{catalyst}$. The results are shown in Table 2. The addition of the Fe and Co metal promoters had a detrimental effect in relation to the methanation reaction in terms of the CH_4 concentration, CO_2 conversion, CH_4 selectivity and CH_4 yield. The decrease is due to the increase in metal deposited upon the catalyst subsequently reducing dispersion, surface area and active metal sites. [34] Aksoylu et al., [29] reported the results of molybdenum loaded on the nickel alumina catalyst for CO_2 methanation in a fixed bed micro reactor made of stainless steel. They reported that suitable amounts of first and second metals are required to obtain an optimum synergetic effect for a molybdenum/nickel alumina catalyst.

The reduction in catalytic activity of the 7 wt.%-Ni Al_2O_3/3 wt.%-Co/Al_2O_3 catalyst may be attributed to the reduction in concentration of the more active nickel metal ion deposited upon the catalyst, subsequently reducing the ability to successfully convert CO_2 and the

hydrogenation process to proceed. While the decrease in the catalytic activity and selectivity with the addition of Fe as a second metal may be attributed to the enhancement of the water gas shift reaction.[35] Tian et al., [36] studied the comparison of monometallic Ni/Al_2O_3 and bimetallic Ni_3Fe/Al_2O_3 catalysts for CO methanation in a fixed bed reactor at different catalyst temperature ranges. It was determined that the monometallic catalyst was more active at higher temperature than the bimetallic catalyst, which was active at lower temperature. They suggested that the catalytic performance of bi-metals is independent of the percentage of individual metal content, but, is dependent on the synergetic effect of the two metals loaded on the support. They also suggested that the synergetic effect is dependent on the quality of alloy formed between the two metallic species upon mixing. Rahmani et al., [37] studied the effect of various metal promoters (Co, La, Ce and Fe) on a Ni/Al_2O_3 catalyst for CO_2 methanation in the temperature range of 200-500 °C. They reported that the catalytic activity of the bimetal catalyst declined at elevated temperature. At lower temperatures some bi-metals (Fe, Ce and La) showed better catalytic activity as compared to the mono-metallic catalyst but at higher temperatures (>300 °C), their methanation activity was reduced. Similarly, Jun et al., [38] studied the effect of various bimetals (Fe, Co, Cu) loaded on a Ni/ZrO_2 catalyst in a high pressure fixed bed reactor in relation to CO_2 methanation. They also concluded that the bimetal catalyst showed better catalytic activity at lower temperature (<250 °C). However, at higher temperature within the range of 300 - 330 °C catalytic activity became stable for both the bimetal and monometallic catalysts. They also concluded that the catalytic activity of a bimetallic catalyst towards CO_2 methanation was greater than a monometallic catalyst at low temperature.

3.8 Influence of catalyst support material

The influence of catalyst support material in the form of SiO_2 and MCM-41 compared to the Al_2O_3 support on the methanation reaction was investigated using 10 wt.% nickel for each support. The catalyst reaction temperature was maintained at 360 °C, the $H_2:CO_2$ ratio was 4:1, the TGHSV was 6000 ml $h^{-1}g^{-1}_{catalyst}$ and the RGHSV was 3000 ml $h^{-1}g^{-1}_{catalyst}$.

Initial characterization of the prepared catalysts was determined using SEM and EDXS metal mapping and the results are shown in Figure 11 and Figure 12 respectively. It was observed that the nickel particles were uniformly dispersed for then 10 wt.%-Ni/Al_2O_3 catalyst compared to the 10 wt.%-Ni/MCM-41 and 10 wt.%-Ni/SiO_2 catalysts. Also, the SEM images

suggest that the particle sizes of the 10 wt.%-Ni/MCM-41 and 10 wt.% Ni/SiO$_2$ catalysts were greater than the 10 wt.%-Ni/Al$_2$O$_3$ catalyst.

The prepared nickel catalysts with the different support materials were also analysed using XRD and the results are shown in Figure 13. In all three of the different reduced nickel-based catalysts, diffraction peaks 2 theta at, 37.4º, 44.3º, 51.68º and 76.24º showed the presence of metallic nickel. Diffraction peaks at 2 theta, 39.2°, 19.14º, 31.6º, 45.5º, 60.34º and 66.42º are represented by the alumina phase related peaks for the 10 wt.%-Ni/Al$_2$O$_3$ catalyst. A single alumina XRD diffraction peak appeared at 60.34º for the 10 wt.%-Ni/MCM-41 catalyst and a silica peak appeared at 25º for the 10 wt.%-Ni/SiO$_2$ catalyst. Quantitative determination of the nickel particle sizes was carried out using the XRD data which showed that the average particle size of the Ni/Al$_2$O$_3$, Ni/MCM-41 and Ni/SiO$_2$ catalysts was, 10.2 nm, 13.7 nm and 28.0 nm, which is consistent with the SEM observations.

The effects of various catalyst support materials on the methanation reaction using 10 wt.% nickel supported on Al$_2$O$_3$, SiO$_2$ and MCM-41 was undertaken. The reaction temperature was maintained at 360 °C and the H$_2$:CO$_2$ ratio was maintained at 4:1 and the TGHSV was 6000 ml h^{-1} g^{-1}$_{catalyst}$ and the RGHSV was 3000 ml h^{-1} g^{-1}$_{catalyst}$. The catalyst calcination temperature used to prepare the catalysts was 950 °C. The results of the methanation experiments in terms of CH$_4$ concentration, CO$_2$ conversion, CH$_4$ selectivity and CH$_4$ yield are shown in Figure 14. The highest catalytic activity was observed with the Ni/Al$_2$O$_3$, catalyst as compared to that of Ni/SiO$_2$ and Ni/MCM-41 catalysts. CO$_2$ conversion with Al$_2$O$_3$, SiO$_2$ and MCM-41 was 82.9 mol.%, 29.6 mol.% and 39.4 mol.% respectively. Also, the maximum methane selectivity was observed with the Al$_2$O$_3$ support which was 97.9%. The catalytic activity of the SiO$_2$ supported catalyst has been suggested to be greatly affected by the presence of water vapor which decreased the amount of carbonyl species which ultimately decreases the methane formation. For example, Aziz et al., [39] investigated the effect of water vapor on the catalytic activity of a 5 wt.%-Ni/MSN catalyst at a temperature of 400 °C using FTIR. They showed that the presence of water vapor results in a decrease in carbonyl species because the water reacts with such species through the water gas shift reaction which results in the formation of CO$_2$. Also, it has been reported that the presence of water favors the sintering of nickel which also inhibits the formation of methane.[39,40] According to a stability analysis conducted by Tatsumi et al., [41] the collapse of the structure of MSN (mesoporous silica nanospheres) support in the presence of water was because of Si-O-Si hydrolysis due to its hydrophilic nature. Carbon dioxide methanation was studied by Du et al., [11] using a 3 wt.%-Ni/MCM-41 catalyst at 300 °C. They reported that the CO$_2$ conversion was very low i.e. a

maximum of up to 10 %. Frontera et al., [40] discussed the results reported by Du et al., [11] and suggested that the lower activity of the MCM-41 catalyst could be attributed to the low catalyst stability of the MCM-41 support in the presence of water which is one of the main products of the methanation reaction

4. CONCLUSIONS

A detailed parametric analysis of the CO_2 methanation reaction in a two-stage reactor system has been investigated. The major conclusions from this study are the following:

1. A suitable total gas hourly space velocity (TGHSV) and reactant gases hourly space velocity (RGHSV) is required for the optimization of the process. Lower RGHSV are favorable for the CO_2 methanation reaction. Higher RGHSV is not suitable because of a lower residence time for the reactant gases to be absorbed on the catalytic surface for the reaction to occur which results in lesser CO_2 conversion.

2. An optimized temperature condition for CO_2 methanation is required to promote the methanation reaction. The maximum CO_2 conversion to CH_4 was observed at 360 °C. However above 360 °C the RWGS becomes dominant and suppresses the methanation reaction.

3. A suitable H_2:CO_2 ratio is required to optimize the maximum methane yield. A stoichiometric ratio close to the ideal stoichiometric ratio of 4:1 showed the maximum CO_2 conversion and methane yield.

4. Ni based catalysts resulted in the maximum activity and selectivity among the metal-alumina catalysts investigated. Because of their catalytic activity over a wide temperature range, nickel-based catalysts are the most suitable catalyst for the methanation reaction.

5. Increased calcination temperature for the preparation of the 10 wt.%-Ni/Al_2O_3 catalyst resulted in the appearance of strong crystalline phases of Ni and alumina which enhanced the activity of catalyst.

6. A suitable amount of metal loading is required for the catalyst to be effective for the CO_2 methanation reaction. Increase in the metal loading up to 10 wt.%, increased the catalytic activity but a further increase to 15%, resulted in a decrease in methane yield because of catalyst sintering and non-uniform metal distribution. Higher nickel loading resulted in the sintering of the catalyst which was evident from XRD data because of the increased crystal sizes of the nickel metal particles with increased loading.

7. The addition of metal promoters to the Ni/Al$_2$O$_3$ catalyst resulted in a decrease in the catalytic activity. The activity of the bi-metallic catalysts is greatly dependent on the synergetic effect between the two metals and is independent of the loading of the 1st or 2nd metal. Therefore, optimised operating conditions and metal loading percentages are required for the synergetic effect to occur.

8. The Al$_2$O$_3$ support showed the maximum activity as compared to SiO$_2$ and MCM-41 for the nickel-based catalysts because of the uniform distribution of Ni metals on the Al$_2$O$_3$ support and resistance to sintering. The XRD data showed that the reduced catalytic activity of Ni on the SiO$_2$ and MCM-41 supports was due to sintering.

REFERENCES

1. Shayan, E.; Zare V.; Mirzaee I. Energ. Convers. Manag. **2018,** 159, 30-41.

2. Li, W.; Wang H.; Jiang X.; Zhu J.; Liu Z.; Guo X.; Song C. RSC Adv., **2018**, 8(14), 7651-7669.

3. Muroyama, H.; Tsuda Y.; Asakoshi T.; Masitah H.; Okanishi T.; Matsui T.; Eguchi K. J. Catal, **2016**, 343, 178-184.

4. Garbarino, G., Riani P.; Magistri L.; Busca G., Int. J. Hydrogen Energ. **2014,** 39(22), 11557-11565.

5. Centi, G.; Perathoner S. Catal. Today, **2009,** 148(3), 191-205.

6. Moghaddam, S.V.; Rezaei M.; Meshkani F.; Daroughegi R. Int. J. Hydrogen Energ. **2018,** 43(34), 16522-16533.

7. Gao, J.; Wang Y.; Ping Y.; D. Hu D.; Xu G.; Gu F.; Su F. RSC Adv. **2012.** 2(6), 2358-2368.

8. Aziz, M.A.A.; Jalil A.A.; Triwahyono S.; Mukti R.R.; Taufiq-Yap Y.H.; Sazegar M.R. Appl. Catal. B-Environ. **2014,** 147, 359-368.

9. Stangeland, K.; Kalai D.Y.; Li H.; Yu Z. Appl. Energ. **2018,** 227, 206-212.

10. Rönsch, S.; Schneider J.; Matthischke S.; Schlüter M.; Götz M.; Lefebvre L.; Prabhakaran P.; Bajohr S. Fuel, 2016, **166**, 276-296.

11. Du, G.; Lim S.; Yang Y.; Wang C.; Pfefferle L.; Haller G.L J. Catal**. 2007,** 249(2), 370-379.

12. Wang, W.; Gong J.; Frontiers Chem. Eng. China, **2011,** 5(1), 2-10.

13. Petala, A.; Panagiotopoulou P. Appl. Catal. B-Environ. **2018,** 224, 919-927.

14. Ma, S.; Song W.; Liu B.; Zheng H.; Deng J.; Zhong W.; Liu J.; Gong X.Q.; Zhao Z. Catal. Sci. Technol. **2016,** 6(15), 6128-6136.

15. Wierzbicki, D.; Debek R.; Motak M.; Grzybek T.; Gálvez M.E.; Da Costa P. Catal. Comm. **2016,** 83, 5-8.

16. Razzaq, R.; Zhu H.; Jiang L.; Muhammad U.; Li C.; Zhang S. Ind.. Eng. Chem. Res. **2013,** 52(6), 2247-2256.

17. Langford, J.I.; Wilson A.J.C. J. Appl. Crystall. **1978.** 11(2), 102-113.

18. Zhou, G.; Liu H.; Cui K.; Jia A.; Hu G.; Jiao Z.; Y. Liu; Zhang X. Appl. Surf. Sci. **2016,** 383, 248-252.

19. Rahmani, S.; Rezaei M.; Meshkani F. J. Ind. Eng. Chem. **2014,** 20(4), 1346-1352.

20. Vita, A.; Italiano C.; Pino L.; Frontera P.; Ferraro M.; Antonucci V.; Appl. Catal. B-Environ. **2018,** 226, 384-395.

21. Abate, S.; Barbera K.; Giglio E.; Deorsola F.; Bensaid S.; Perathoner S.; Pirone R.; Centi G. Ind. Eng. Chem. Res. **2016,** 55(30), 8299-8308.

22. Ocampo, F., Louis B.; Roger A.C. Appl. Catal. A-Gen. **2009,** 369(1), 90-96.

23. Moghaddam, S.V.; Rezaei M.; Meshkani F.; Daroughegi R. Int. J. Hydrogen Energ. **2018,** 43(41), 19038-19046.

24. Jia, X.; Zhang X.; Rui N.; Hu X.; Liu C.J. Appl. Catal. B-Environ. **2019,** 244, 159-169.

25. Zhou, L.; Wang Q.; Ma L.; Chen J.; Ma J.; Zi Z. Catal. Lett. **2015,** 145(2), 612-619.

26. Lu, B.; Kawamoto K**. Fuel, 2013**, 103, 699-704.

27. Aziz, M.A.A.; Jalil A.A.; Triwahyono S.; Sidik S.M. Appl. Catal. A-Gen. **2014,** 486, 115-122.

28. Razzaq, R.; Li C.; Usman M.; Suzuki K.; Zhang S. Chem. Eng. J. **2015,** 262, 1090-1098.

29. Aksoylu, A.E.; Mısırlı Z.; Önsan Z.I. Appl. Catal. A-Gen. **1998,** 168(2), 385-397.

30. Burger, T.; Koschany F.; Thomys O.; Köhler K.; Hinrichsen O. Appl. Catal. A-Gen. **2018**, 558, 44-54.

31. Gao, J.; Jia C.; Li J.; Zhang M.; Gu F.; Xu G.; Zhong Z.; Su F. J. Energ. Chem. **2013**, 22(6), 919-927.

32. Daroughegi, R.; Meshkani F.; Rezaei M. Int. J. Hydrogen Energ. **2017,** 42(22), 15115-15125.

33. Zhen, W.; Li B.; Lu G.; Ma J. Chem. Comm. **2015**, 51(9), 1728-1731.

34. Gao, J., Liu Q.; Gu F.; Liu B.; Zhong Z.; Su F. RSC Adv. **2015,** 5(29), 22759-22776.

35. Kang, S.H.; Ryu J.H.; Kim J.H.; Seo S.J.; Yoo Y.D.; Sai Prasad P.S.; Lim H.J.; Byun C.D. Korea. J. Chem. Eng. **2011,** 28(12), 2282-2286.

36. Tian, D.; Liu Z.; Li D.; Shi H.; Pan W.; Cheng Y. Fuel, **2013**, 104, 224-229.

37. Rahmani, S.; Meshkani F.; Rezaei M. Environ. Prog. Sus. Energ. (**https://doi.org/10.1002/ep.13040**) **2018**.

38. Ren, J.; Qin X; Yang J.Z.; Qin Z.F.; Guo H.L.; Lin J.Y.; Li Z. Fuel Proc. Technol. **2015,** 137, 204-211.

39. Aziz, M.A.A.; Jalil A.A.; Triwahyono S.; Saad M.W.A. Chem. Eng. J. **2015,** 260, 757-764.

40. Frontera, P.; Macario A.; Ferraro M.; Antonucci P. Catalysts, **2017,** 7(2), 59.

41.   Tatsumi, T.; Koyano K.A.; Tanaka Y.; Nakata S. J. Porous Mat. **1999,** 6(1), 13-17.
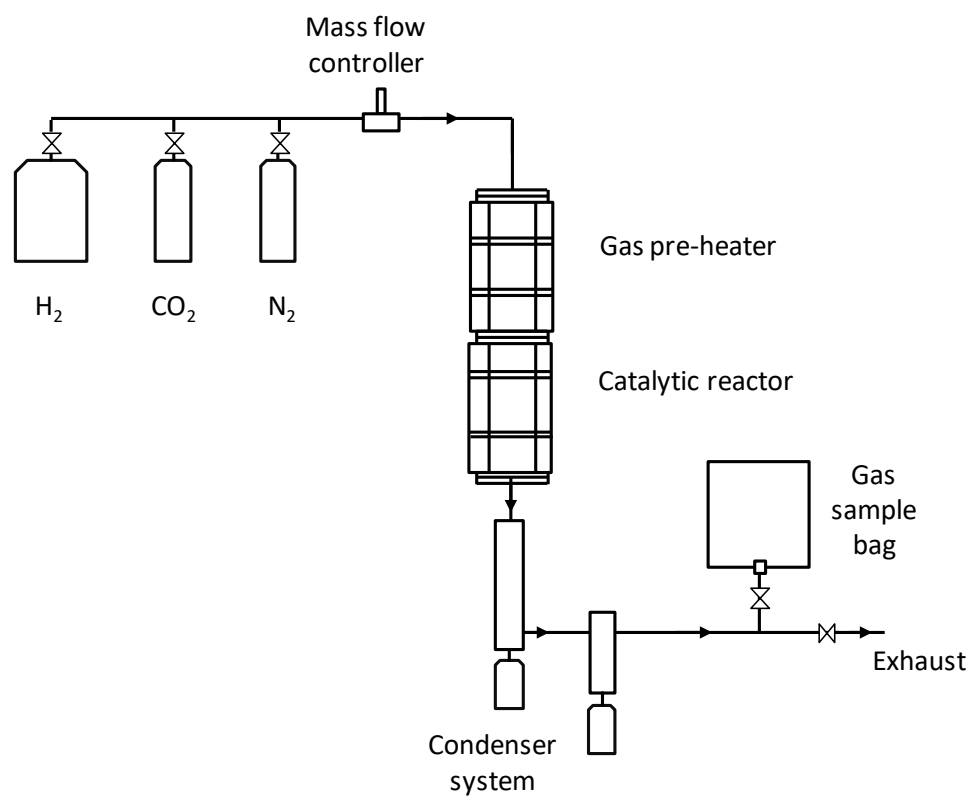
Figure Captions

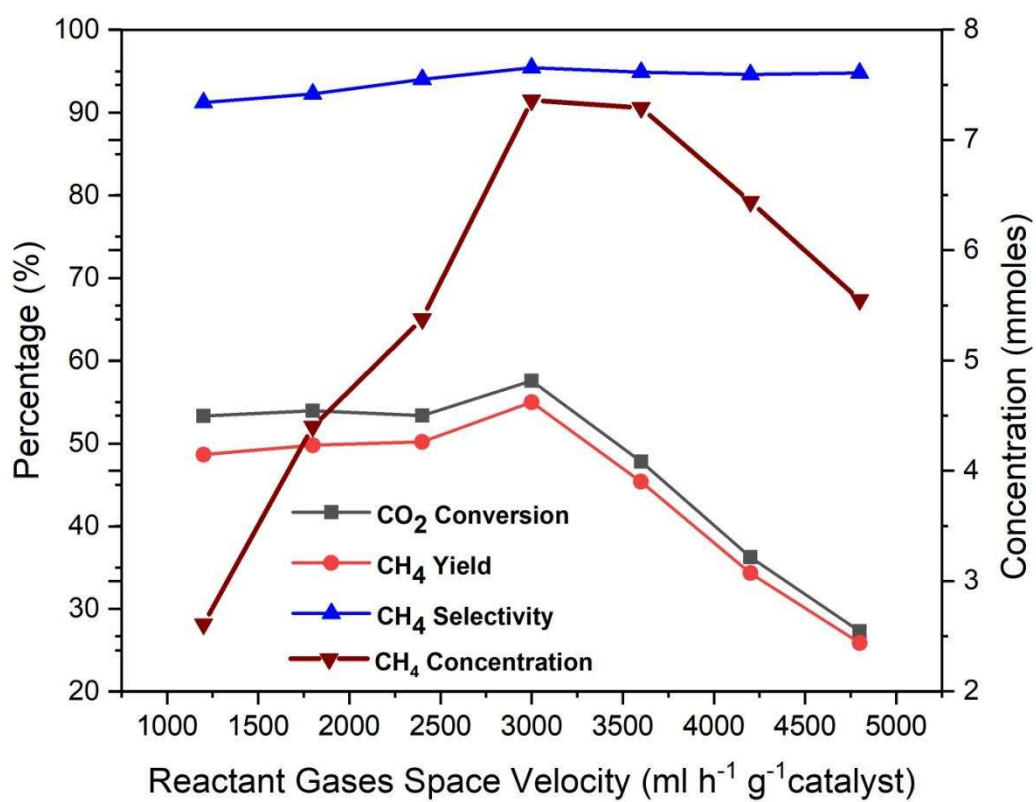**Figure 1.** Schematic diagram of the methanation reactor.

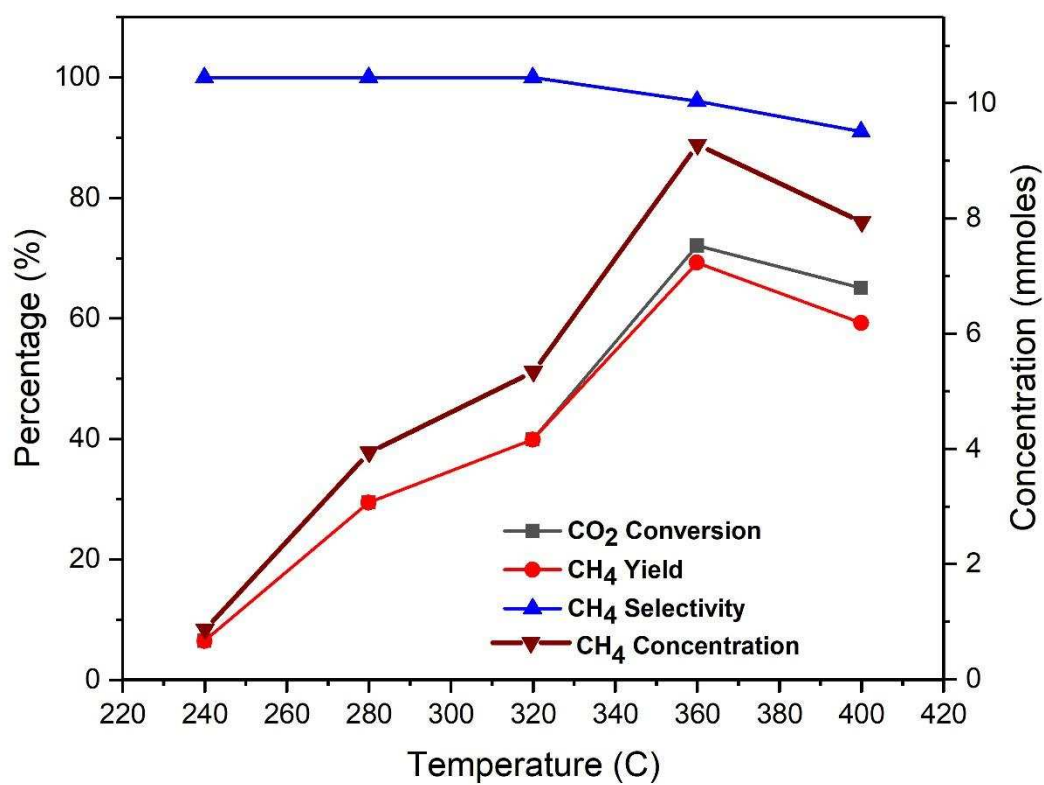**Figure 2.** Effect of reactant gas flow rates on CH_4 concentration, CO_2 conversion, CH_4 selectivity and CH_4 yield.

Figure 3. Effect of catalyst temperature on CH_4 concentration, CO_2 conversion, CH_4 selectivity and CH_4 yield.

Figure 4. Effect of H_2/CO_2 ratio on CH_4 concentration, CO_2 conversion, CH_4 selectivity and CH_4 yield.
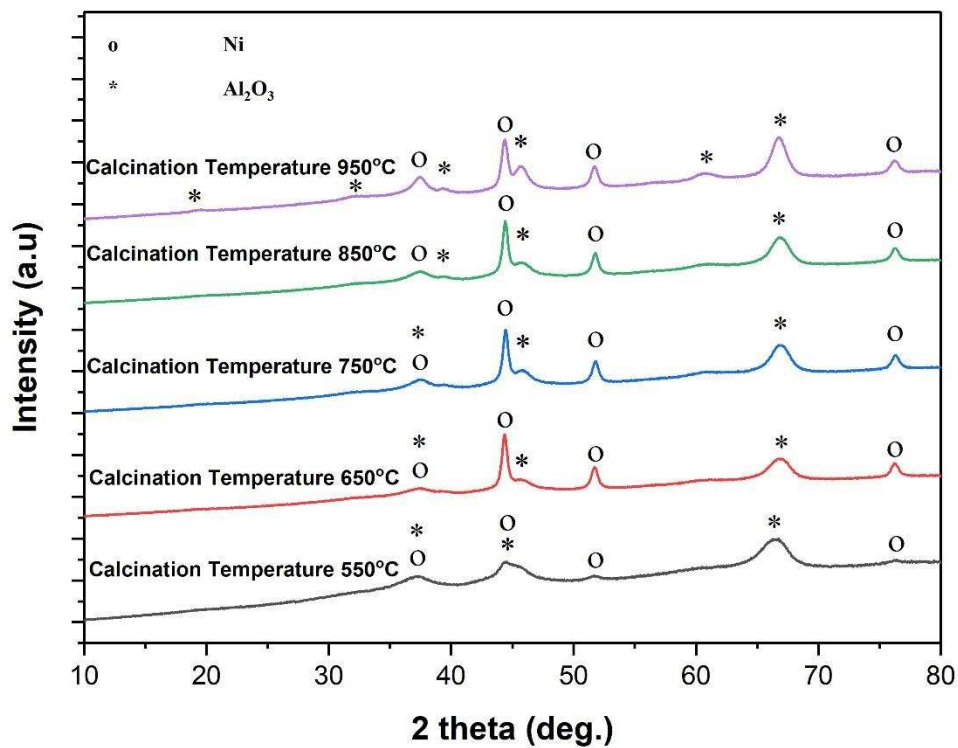
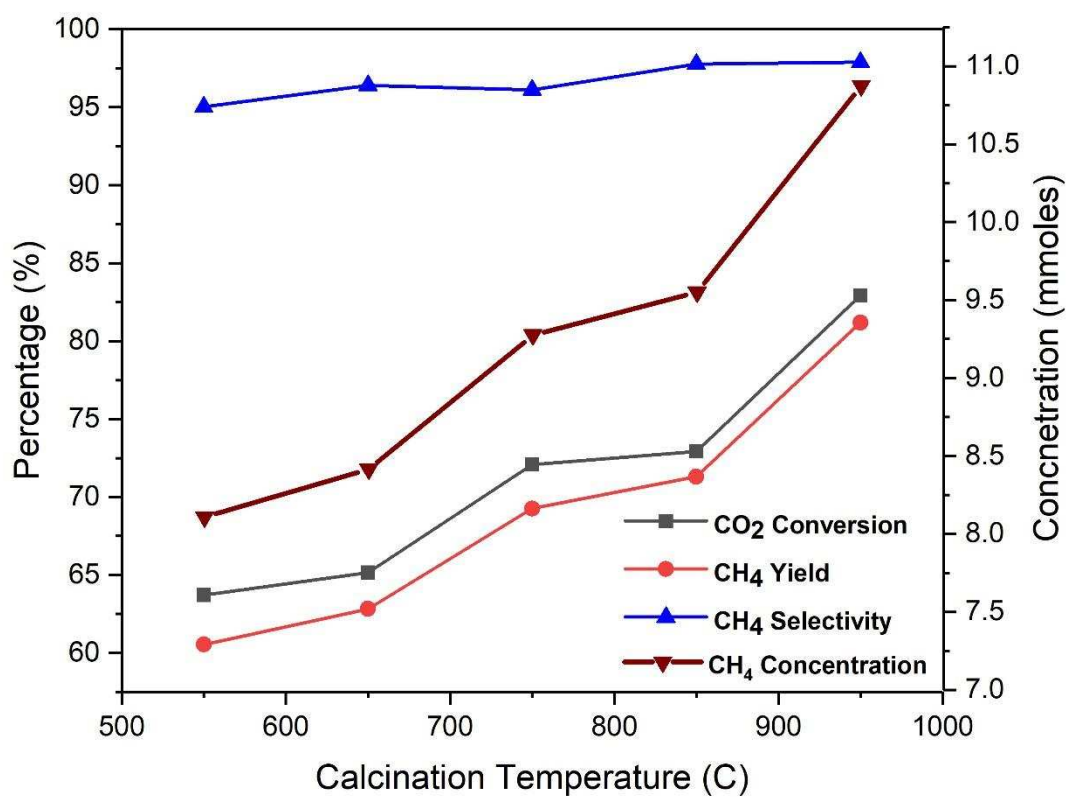**Figure 5.** XRD patterns of 10 wt.%-Ni/Al_2O_3 calcined at different temperature.

Figure 6 Effect of calcination temperature on CH_4 concentration, CO_2 conversion, CH_4 selectivity and CH_4 yield.
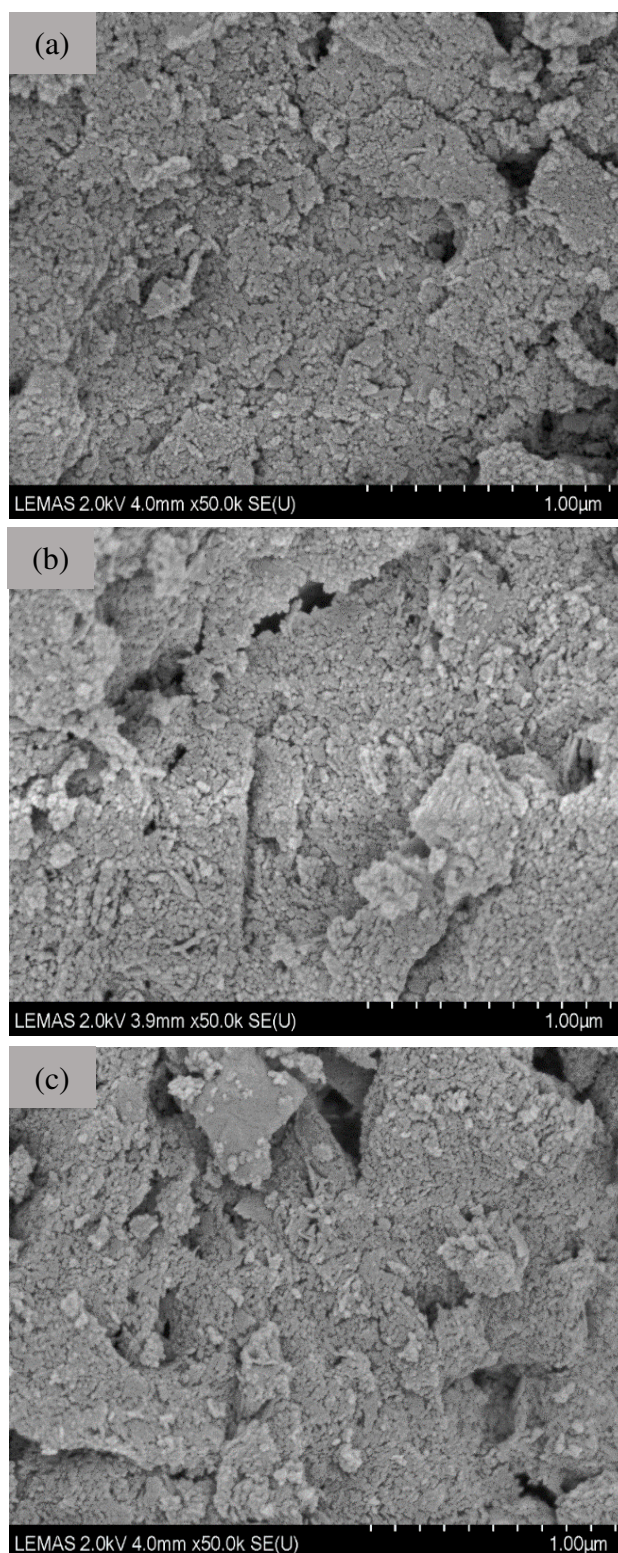
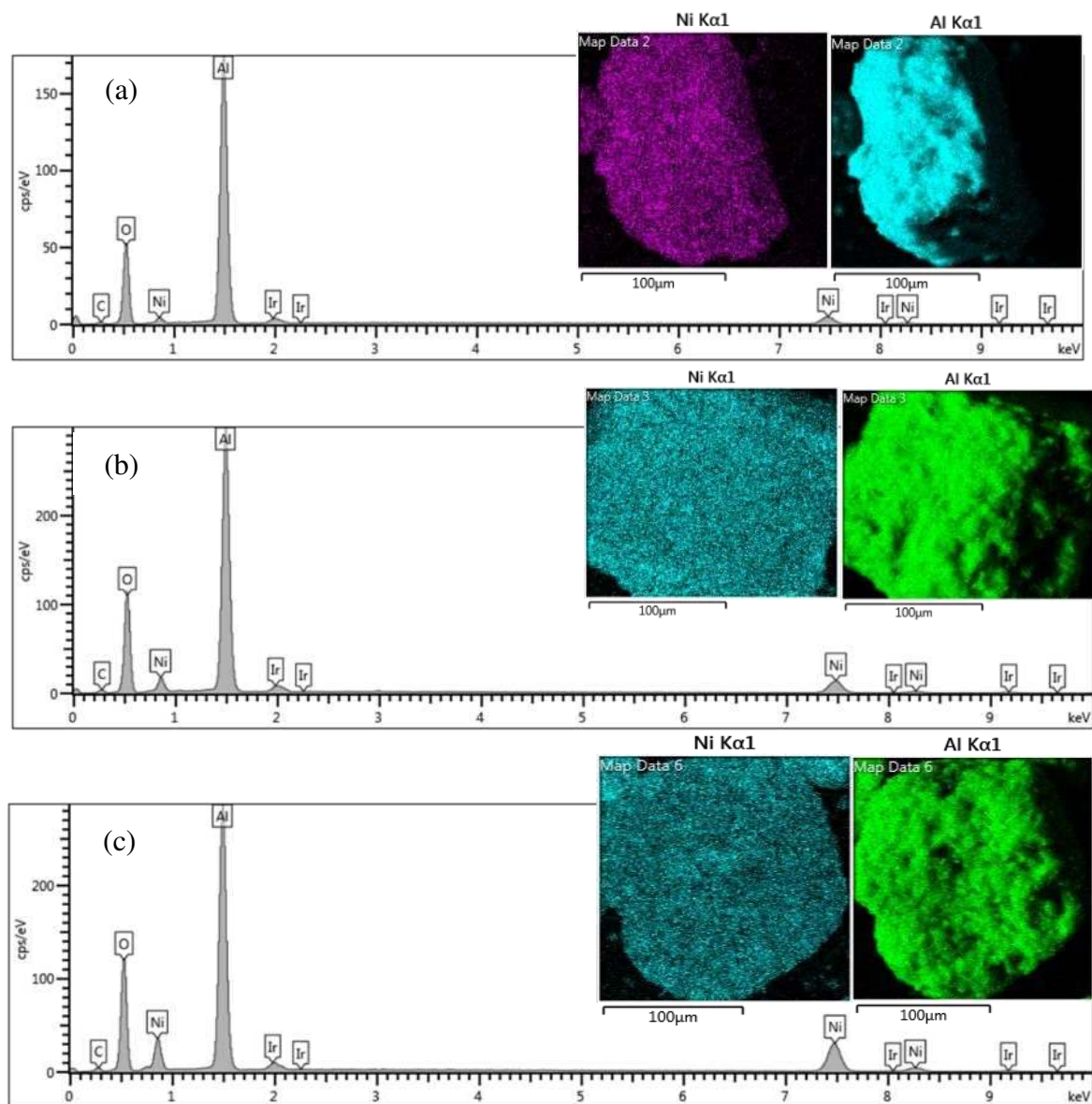**Figure 7.** SEM analysis of nickel loadings on alumina support a) 5 wt.%-Ni/Al_2O_3 b) 10 wt.%/Al_2O_3 c) 15 wt.%-Ni/Al_2O_3.

Figure 8. EDXS mapping of different nickel loadings on alumina support a) 5 wt.%-Ni/Al_2O_3 b) 10 wt.%/Al_2O_3 Ni c) 15 wt.%-Ni/Al_2O_3.

Figure 9. XRD patterns of various nickel loadings on alumina support.

Figure 10. Effect of metal loading on CH_4 concentration, CO_2 conversion, CH_4 selectivity and CH_4 yield.

Figure 11. SEM patterns of different supports a) 10 wt.%-Ni/SiO_2 b) 10 wt.%-Ni/MCM-41 c) 10 wt.%-Ni/Al_2O_3.

Figure 12. EDXS mapping of different supports a) 10 wt.%-Ni/SiO_2 b) 10 wt.%-Ni/MCM-41 c) 10 wt.%-Ni/Al_2O_3.

Figure 13. XRD patterns of different supports a) 10 wt.%-Ni/SiO_2 b) 10 wt.%-Ni/MCM-41 c) 10 wt.%-Ni/Al_2O_3.

Figure 14. Effect of support on CH_4 concentration, CO_2 conversion, CH_4 selectivity and CH_4 yield.

Figure 1. Schematic diagram of the methanation reactor.

Figure 2. Effect of reactant gas flow rates on CH_4 concentration, CO_2 conversion, CH_4 selectivity and CH_4 yield.

Figure 3 Effect of catalyst temperature on CH_4 concentration, CO_2 conversion, CH_4 selectivity and CH_4 yield.

Figure 4 Effect of H$_2$/CO$_2$ ratio on CH$_4$ concentration, CO$_2$ conversion, CH$_4$ selectivity and CH$_4$ yield.

Figure 5. XRD patterns of 10 wt.%-Ni/Al$_2$O$_3$ calcined at different temperature.

Figure 6. Effect of calcination temperature on CH_4 concentration, CO_2 conversion, CH_4 selectivity and CH_4 yield.

Figure 7. SEM analysis of nickel loadings on alumina support a) 5 wt.%-Ni/Al$_2$O$_3$ b) 10 wt.%/Al$_2$O$_3$ c) 15 wt.%-Ni/Al$_2$O$_3$.

Figure 8. EDXS mapping of different nickel loadings on alumina support a) 5 wt.%-Ni/Al$_2$O$_3$ b) 10 wt.%/Al$_2$O$_3$ Ni c) 15 wt.%-Ni/Al$_2$O$_3$.

Figure 9. XRD patterns of various nickel loadings on alumina support.

Figure 10. Effect of metal loading on CH$_4$ concentration, CO$_2$ conversion, CH$_4$ selectivity and CH$_4$ yield.
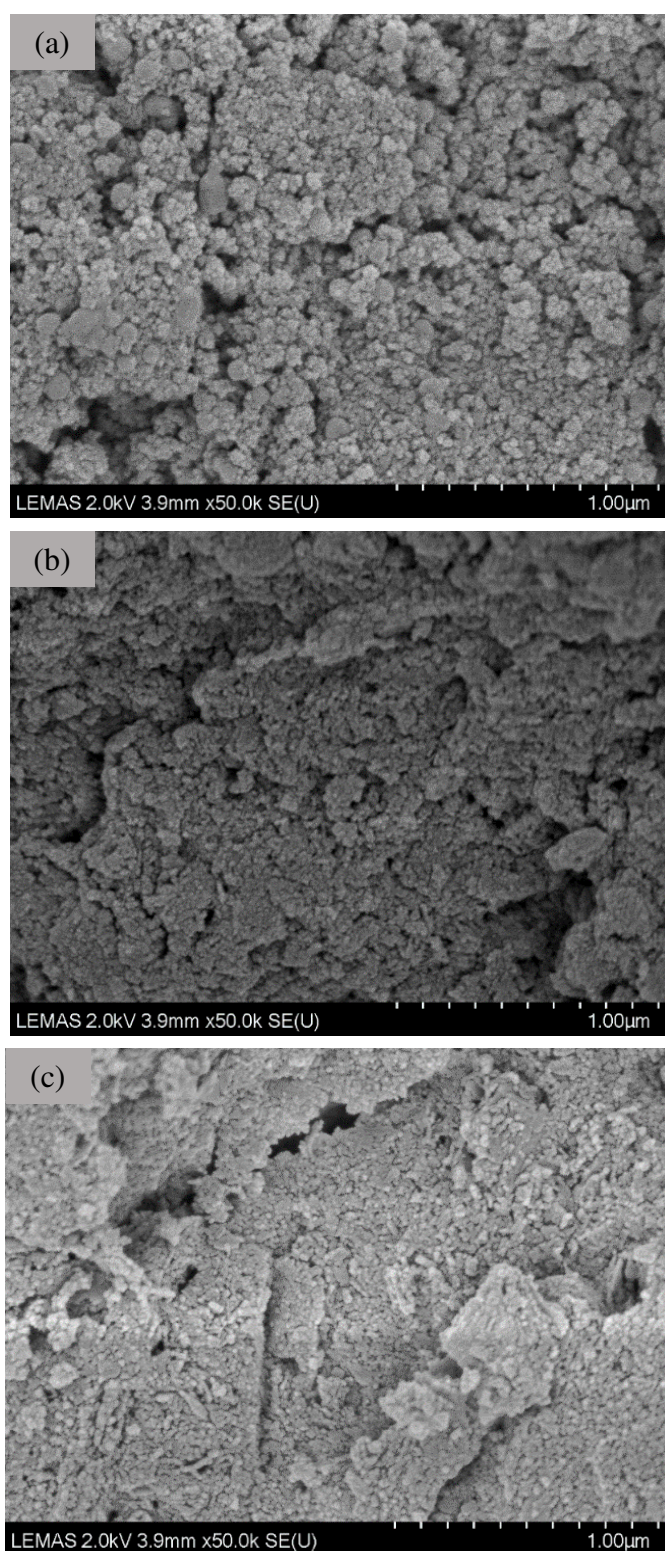
Figure 11. SEM patterns of different supports a) 10 wt.%-Ni/SiO$_2$ b) 10 wt.%-Ni/MCM-41 c) 10 wt.%-Ni/Al$_2$O$_3$.
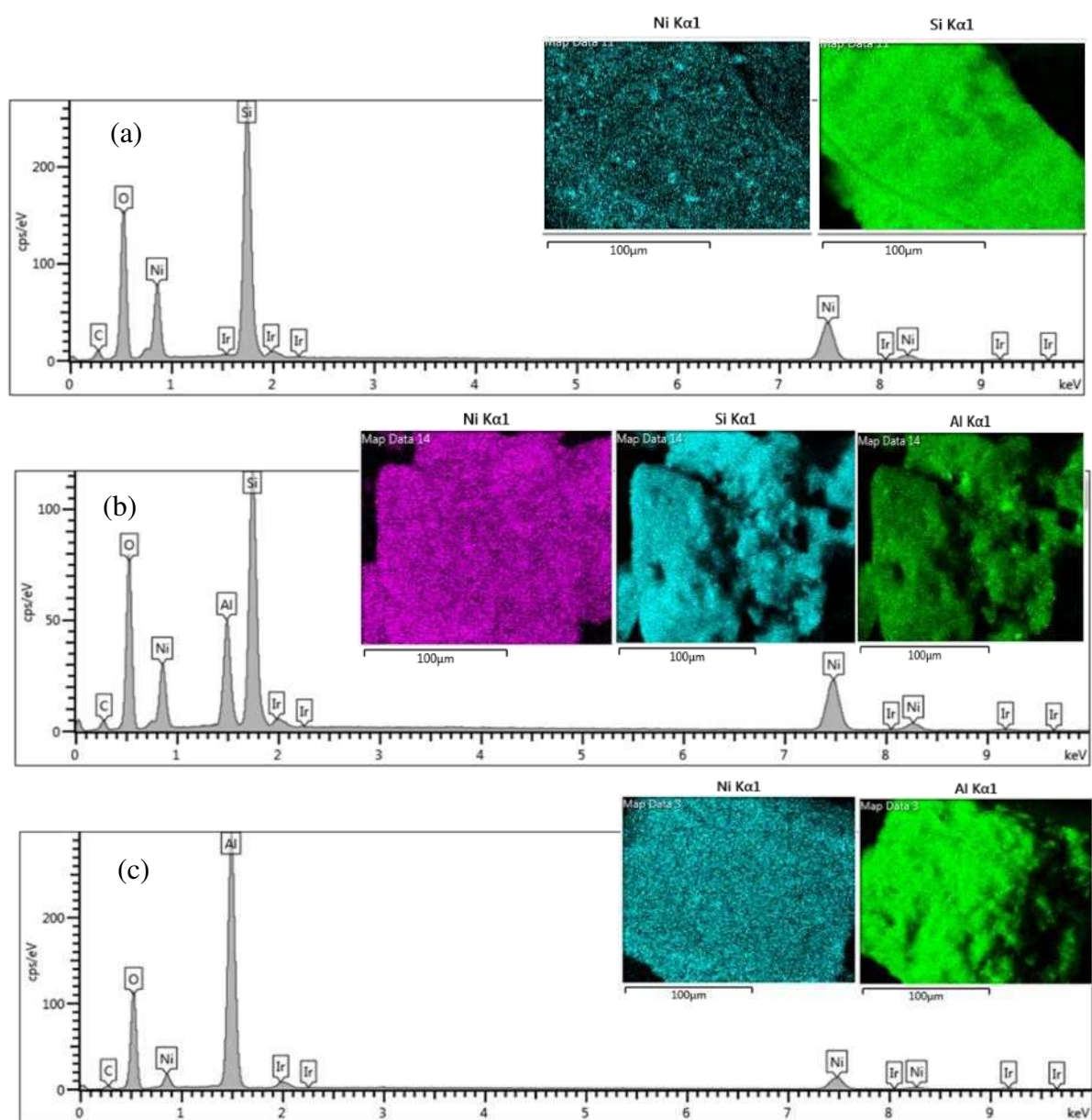
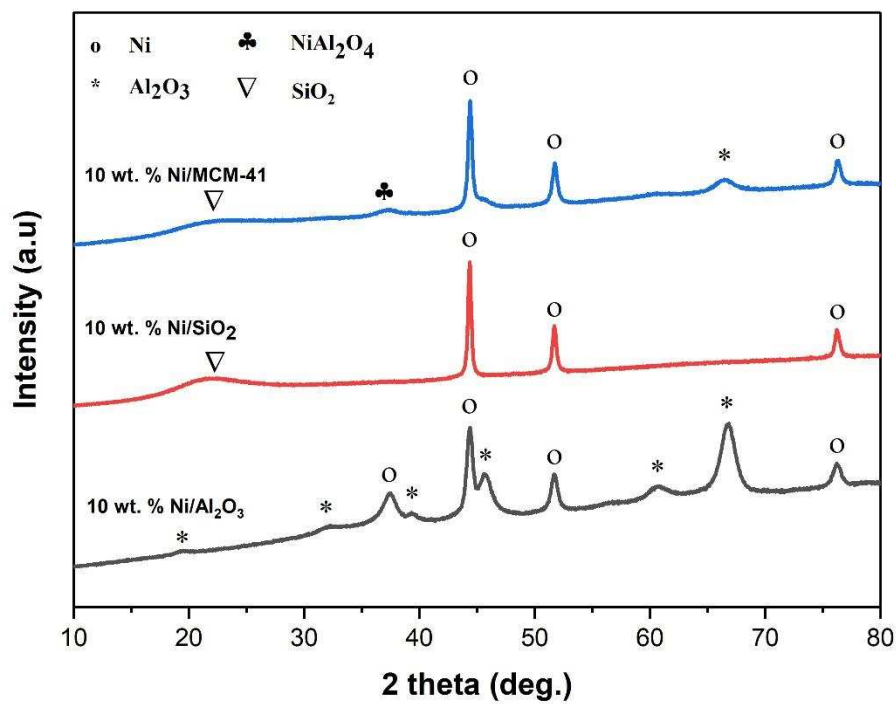**Figure 12.** EDXS mapping of different supports a) 10 wt.%-Ni/SiO$_2$ b) 10 wt.%-Ni/MCM-41 c) 10 wt.%-Ni/Al$_2$O$_3$.

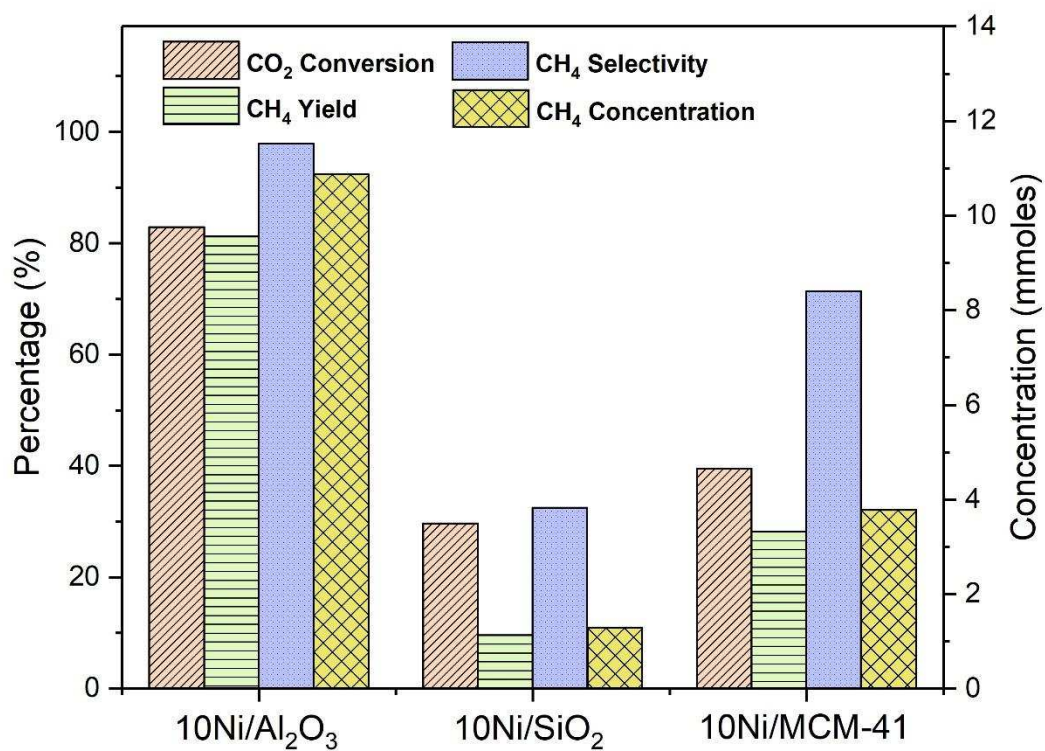**Figure 13.** XRD patterns of different supports a) 10 wt.%-Ni/SiO$_2$ b) 10 wt.%-Ni/MCM-41 c) 10 wt.%-Ni/Al$_2$O$_3$.

Figure 14. Effect of support on CH_4 concentration, CO_2 conversion, CH_4 selectivity and CH_4 yield.

Table 1. Effect of metals on CH₄ concentration, CO₂ conversion, CH₄ selectivity and CH₄ yield.

Catalyst	CO_2 Conversion (%)	CH_4 Concentration (mmole)	CH_4 Yield (%)	CH_4 Selectivity (%)
10 wt.%-Ni/Al$_2$O$_3$	72.1	9.2	69.3	96.1
10 wt.%-Fe/Al$_2$O$_3$	9.7	0.02	0.1	1.2
10 wt.%-Co/Al$_2$O$_3$	50.3	5.5	40.7	81.1
10 wt.%-Mo/Al$_2$O$_3$	8.4	3.6	0.3	3.2

Table 2. Effect of metal promotors on CH_4 concentration, CO_2 conversion, CH_4 selectivity and CH_4 yield.

Catalyst	CO_2 Conversion (mol. %)	CH_4 Concentration (mmol)	CH_4 Yield (mol. %)	CH_4 Selectivity (%)
$10Ni/Al_2O_3$	83.0	10.9	81	98
$10Ni/3Fe/Al_2O_3$	51.7	6.3	47	92
$10Ni/3Co/Al_2O_3$	60.5	7.7	58	95
$7Ni/3Co/Al_2O_3$	71.0	9.0	68	96
$10Ni/1Co/Al_2O_3$	75.0	9.9	73	98